Advantages of a mobile LSPIV method for measuring flood discharges and improving stage-discharge curves

Guillaume Dramais, J. Le Coz, B. Camenen, A. Hauet

Author-produced version of the article published in Journal of Hydro-environment Research 5 (2011) 301-312
The original publication is available at http://www.sciencedirect.com, doi:10.1016/j.jher.2010.12.005

Advantages of a mobile LSPIV method for measuring flood discharges and improving stage-discharge curves

Guillaume Dramais[1,*], Jérôme Le Coz[1], Benoît Camenen[1], and Alexandre Hauet[2]

[*]Corresponding author. Tel: +33 (0)472 208 771, Fax: +33 (0)478 477 875 guillaume.dramais@cemagref.fr

[1]Cemagref, HHLY, Hydrology-Hydraulics, 3 bis quai Chauveau, 69336 Lyon, France

[2]EDF-DTG, CHPMC, 62 bis rue Raymond IV, 31000 Toulouse, France

Abstract

This paper investigates the potential of fast flood discharge measurements conducted with a mobile LSPIV device. LSPIV discharge measurements were performed during two hydrological events on the Arc River, a gravel-bed river in the French Alps: a flood greater than the 10 year return period flood in May, 2008, and a reservoir flushing release in June, 2009. The mobile LSPIV device consists of a telescopic mast with a remotely controlled platform equipped with a video camera. The digital video camera acquired sequences of images of the surface flow velocities. Ground Reference Points (GRPs) were positioned using a total station, for further geometrical correction of the images. During the flood peak, surface flow velocities up to 7 m/s and large floating objects prevented any kind of intrusive flow measurements. For the computation of discharge, the velocity coefficient was derived from available vertical velocity profiles measured by current meter. The obtained value range (0.72 – 0.79) is consistent with previous observations at this site and smaller than the usual default value (0.85) or values observed for deeper river sections (0.90 typically). Practical recommendations are drawn. Estimating stream discharge in high flow conditions from LSPIV measurements entails a complex measurement process since many parameters (water level, surface velocities, bathymetry, velocity coefficient, etc.) are affected by uncertainties and can change during the experiment. Sensitivity tests, comparisons and theoretical considerations are reported to assess the dominant sources of error in such measurements. The multiplicative error induced by the velocity coefficient was confirmed to be a major source of error compared with estimated errors due to water level uncertainty, free-surface deformations, number of image pairs, absence or presence of artificial tracers, and cross-section bathymetry profiles. All these errors are estimated to range from 1%-5% whereas the velocity coefficient variability may be 10%-15% according to the site and the flow characteristics. The analysis of 36 LSPIV sequences during both events allowed the assessment of the flood discharges with an overall uncertainty less than 10%. A simple hydraulic law based on the geometry of the three sills of the Pontamafrey gauging station was proposed instead of the existing curve that is fitted on available gauging data. The high flow LSPIV discharge measurements indicated that this new curve is more accurate for high discharges since they are evenly distributed in a ±10% interval around it. These results demonstrate the interest of the remote stream gauging techniques together with hydraulic analysis for improving stage-discharge relationships and reducing uncertainties associated with fast flood discharges.

Keywords

LSPIV, flood discharge, river gauging, stage-discharge curves

Author-produced version of the article published in Journal of Hydro-environment Research 5 (2011) 301-312
The original publication is available at http://www.sciencedirect.com, doi:10.1016/j.jher.2010.12.005

1 Introduction

All around the world, hydrometry teams face difficulties in measuring flood discharge. Conventional methods and instruments for stream gauging measurement involve deployment in the river with a boat or sensors. Remote methods are safer and easier options for measuring flood discharge. In recent years, radar (Costa et al., 2006) and image-based (Fujita et al., 1998, Muste et al., 2009) velocity measurements have been used in a range of flow conditions. As one of the remote image-based techniques, the Large Scale Particle Image Velocimetry (LSPIV) was tested against two-dimensional depth-averaged calculations (Jodeau et al., 2008), flow rate calculated with stage-discharge curve (Hauet et al., 2008b), or ADCP measurements (Le Coz et al., 2010).

In this article, the objective is to assess the uncertainty in the measurement of a flood discharge conducted with a mobile LSPIV system at a given river site. This kind of device documented by Kim et al. (2008) can be used to study ungauged rivers or several points throughout a river catchment during a hydrological event. Estimating stream discharge in high flow conditions from LSPIV measurements entails a complex measurement process since many parameters (water level, surface velocities, bathymetry, velocity coefficient, etc.) are affected by uncertainties and can change during the experiment. We explore in this study some specific constraints and errors for mobile LSPIV measurements: (i) Velocity coefficient; (ii) Water level and orthorectification (iii) Waves and free-surface deformation; (iv) Image pair sampling; (iii) Use of artificial tracers; (v) Cross-section bathymetry.

This study investigates two hydrological events on the Arc River, a gravel bed river located in the French Alps: (1) a flood greater than a 10-year return period flood in May, 2008, and (2) a reservoir flushing release in June, 2009. The May 2008 major flood caused some damage and residents had to be evacuated.

This set of field data improves the knowledge and the uncertainty estimation of flood discharge measurement with a mobile LSPIV system. From sensitivity tests and the comparison of LSPIV discharges with concurrent discharge measurement, main uncertainty sources are evaluated, and practical recommendations are drawn. In particular, the potential of the mobile LSPIV stream gauging technique for improving the highest or extrapolated part of stage-discharge curves is demonstrated.

2 Material and methods

2.1 LSPIV technique applied to discharge measurements

Since the seminal work of Fujita et al. (1998), the application of the Particle Image Velocimetry (PIV) technique (Adrian, 1991) to large-scale parts of the free-surface of flume and field open-channel flows has been disseminated widely and successfully in the hydraulic research and engineering community (Muste et al. 2010, this issue). The Large-Scale PIV (LSPIV) entails five steps : illumination, seeding, recording, ortho-rectification and processing (cf. e.g. Muste et al. 2009 for a detailed review of the technique).

The discharge through a given bathymetry profile located within a time-averaged LSPIV surface velocity field may be computed following the standard velocity-area method for surface float measurements (ISO 748, 2007). The bathymetry profile needs to be measured using conventional methods before or after the flood. If morphological changes are likely to occur, it is better to measure it both before and after the flood, or even during the flood. For example, some remote bathymetry measurements using a Ground Penetrating Radar were tested by Costa et al. (2006). Depth-averaged velocities at each node of the bathymetry transect need to be computed through i) interpolation or

Author-produced version of the article published in Journal of Hydro-environment Research 5 (2011) 301-312
The original publication is available at http://www.sciencedirect.com, doi:10.1016/j.jher.2010.12.005

extrapolation of the surrounding LSPIV surface velocities and ii) multiplication by a velocity coefficient accounting for the vertical velocity distribution (Le Coz et al., 2010).

2.2 Mobile LSPIV system

The mobile LSPIV system consists of a digital video camera (Canon MV750i) set either on a conventional tripod, or on a mobile telescopic mast (Fireco components) whose height can be set from 2 to 10 m. The camera was remotely controlled from the ground, in order to adjust view angles. Pictures can be acquired on electromagnetic tape (mini-DV) or directly with a laptop connected via an IEEE 1394 interface. Image resolution was 720 x 576, acquisition time is about 2 minutes per sequence, at a rate of 25 frames per second.

For each test, several GRPs were positioned along both banks of the river. White and red 50 cm by 50 cm square targets were used to identify the GRP in the sequences. For the cross section topography, the GRP coordinate measurements, and all water level measurements, a total station (Leica TC305) and a DGPS system (Leica GPS1200) were used following standard protocols. Throughout this study, the elevation is expressed in meters above sea level, in the French NGF metric system (Nivellement Général de la France).

The water colour was very dark due to very high concentrations of fine suspended sediment, greater than ~10 g/L. White artificial tracers contrasting in colour with the water free-surface were used to improve the detection of flow movement. Such tracers were Ecofoam chips, a biodegradable, water soluble foam filled material created from wheat. The chips create visible patterns on the water surface and can improve the quality of calculations by the LSPIV algorithm.

2.3 Sensitive parameters and associated errors

Estimating stream discharge in high flow conditions from LSPIV measurements entails a complex measurement process. Many measured or estimated parameters are affected by uncertainties and may show a significant variability in space and time. The sources of error in LSPIV measurements have been described (cf. e.g. Muste et al., 2009, Kim et al., 2008). Hauet et al. (2008a) also provided a useful sensitivity analysis of LSPIV error sources using a numerical simulator. However, further experimental tests are still required to assess the quality of LSPIV discharges, and to prepare the building of a complete uncertainty analysis methodology.

The present study case aims at exploring the potential error sources in flood discharge measurements using a mobile LSPIV system (Kim et al., 2008). Some of these error sources are common to all LSPIV measurements, such as the number of image pairs considered to establish the time-averaged velocity field, or the mean value and variability of the site-specific velocity coefficient (Jodeau et al., 2008, Le Coz et al., 2010). In a LSPIV discharge measurement conducted during a flood at a given site with a mobile system, specific error sources arise from technical constraints and the nature of the flow. In particular, the choice of the image view point and the topographic measurements of the GRP, the water levels and the cross-sectional bathymetry profiles are usually difficult in flood conditions.

During the LSPIV and flow measurement process, if the water level is underestimated, horizontal distances are exaggerated (Fig.1), hence velocities will be overestimated. However, the wetted area is also affected and the discharge result is reduced. Inversely, when the water level is overestimated, velocities decrease and the wetted area increases. Due to opposite effects of the water level error on the velocity and wetted area computations, the final discharge result could be compensated but false.

Author-produced version of the article published in Journal of Hydro-environment Research 5 (2011) 301-312
The original publication is available at http://www.sciencedirect.com, doi:10.1016/j.jher.2010.12.005

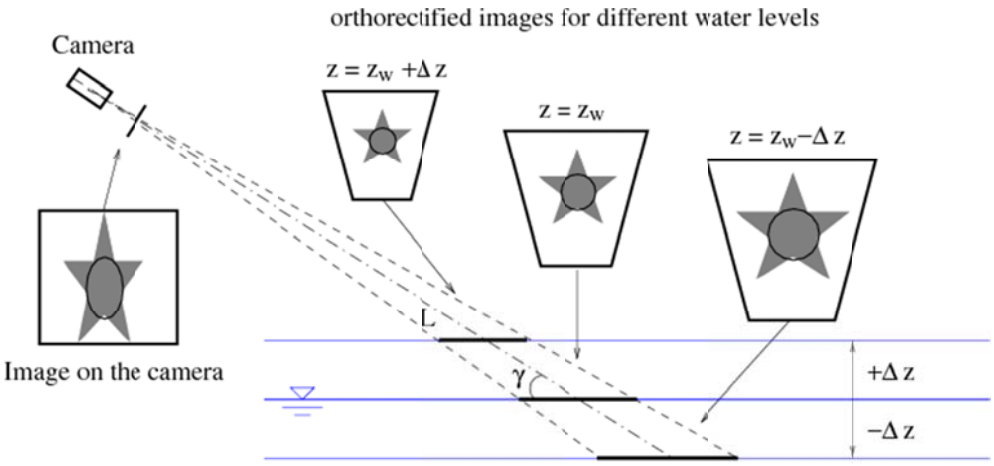

Fig.1 Effect of a water level error on the metric size of orthorectified pixels, hence on the surface velocities.

Waves and other deformations may also affect the free-surface in supercritical flows. Resulting errors in the image orthorectification process may be detrimental to the results as the magnitude, orientation and position surface velocities may be significantly distorted. LSPIV velocity measurements during floods may also be affected by poorly contrasted flow tracers and almost stationary patterns such as sun reflections on stationary waves. One can improve the displacement detection using artificial tracers as was done in this study. Last, the velocity of surface tracers may be not representative of the real velocity of the flow (Hauet et al., 2008b), due to wind, surface waves or diffusion effects. However, such effects are usually negligible in our case with fast flood flows.

3 Study case

3.1 The Arc River

The Arc River is a torrential, gravel-bedded river of the French Alps with a catchment area of 1957 km² (Fig.2a). Since the Middle Ages, the active width of the initially wide braided stream has been continuously reduced (Marnézy, 1999). Human communities, industrial activities, and transportation networks have been concentrated in the restricted and constrained spatial domain of the narrow valley. The main road, highway and railway to Italy are along this river. The construction of the highway in the 1990s gave its present aspect to the Lower Arc River, mostly as straight reaches guided by 50m-spaced rip-rap dykes, with bed slope ranging from 0.5% to 6% (Hydratec and Cemagref, 1999).

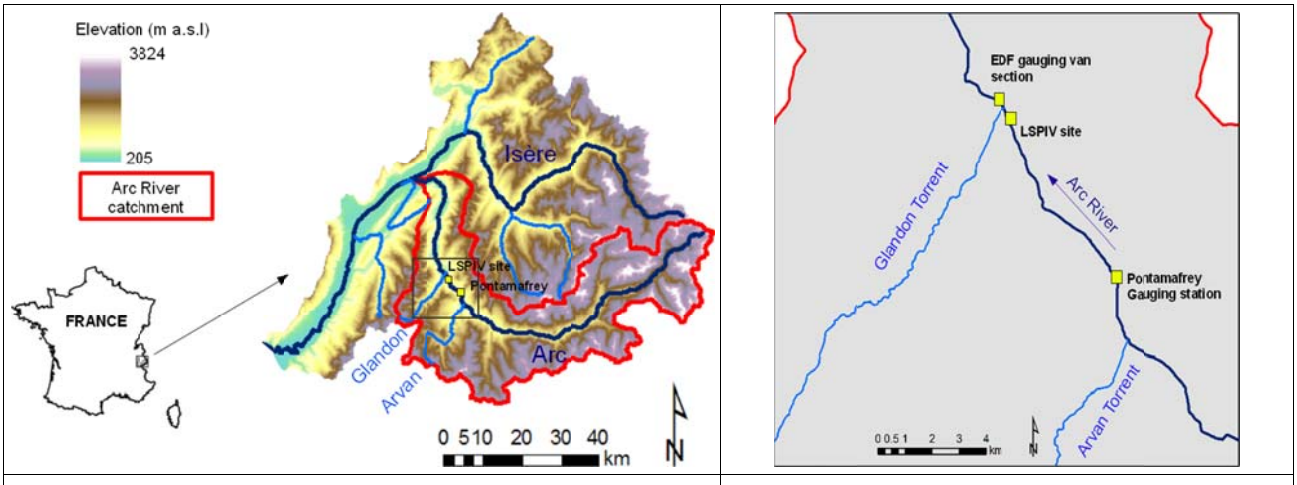

(a) (b)

Fig.2 Location map of the Arc river system (a), and a close view of the reach between Pontamafrey

Author-produced version of the article published in Journal of Hydro-environment Research 5 (2011) 301-312
The original publication is available at http://www.sciencedirect.com, doi:10.1016/j.jher.2010.12.005

gauging station and the LSPIV site (b).

Natural flood peak discharge percentiles computed by Cemagref and EDF (1998) are 260 m³/s (2-year return period), 340 m³/s (5-year return period), 400 m³/s (10-year return period), 520 m³/s (25-year return period), 675 m³/s (50-year return period), and 900 m³/s (100-year return period).

3.2 Test site for mobile LSPIV measurements

LSPIV experiments took place in a straight reach of the Arc river, with a mean longitudinal bed slope of 0.3% (Jodeau et al., 2008). This LSPIV test site is located 7 km downstream of the reference gauging station at Pontamafrey (Fig.2b). On the right upstream side of the bridge, a gauging station has been operated by Cemagref since 2005. The water level is measured by a reliable pneumatic pressure gauge (Nimbus, Ott) the instantaneous data was recorded every 30 minutes. The accuracy of the water level was controlled at each visit on the site (every 2 months) with an optical level (Wild Na20). The observed drift was +/- 1cm. A GSM modem allows data transmission to the office for the survey and the recording in the database.
The camera was installed on the left bank, downstream the bridge (Fig.3a), with a very low angle between the camera viewpoint and the horizontal (site angle). Other viewpoints were more difficult and most often perifluvial vegetation blocked the camera shots. The camera recorded images of the river downstream of the bridge. Unfortunately, the bridge has one central pier, which induced some perturbation of the flow and of the bed profile in both upstream and downstream directions.

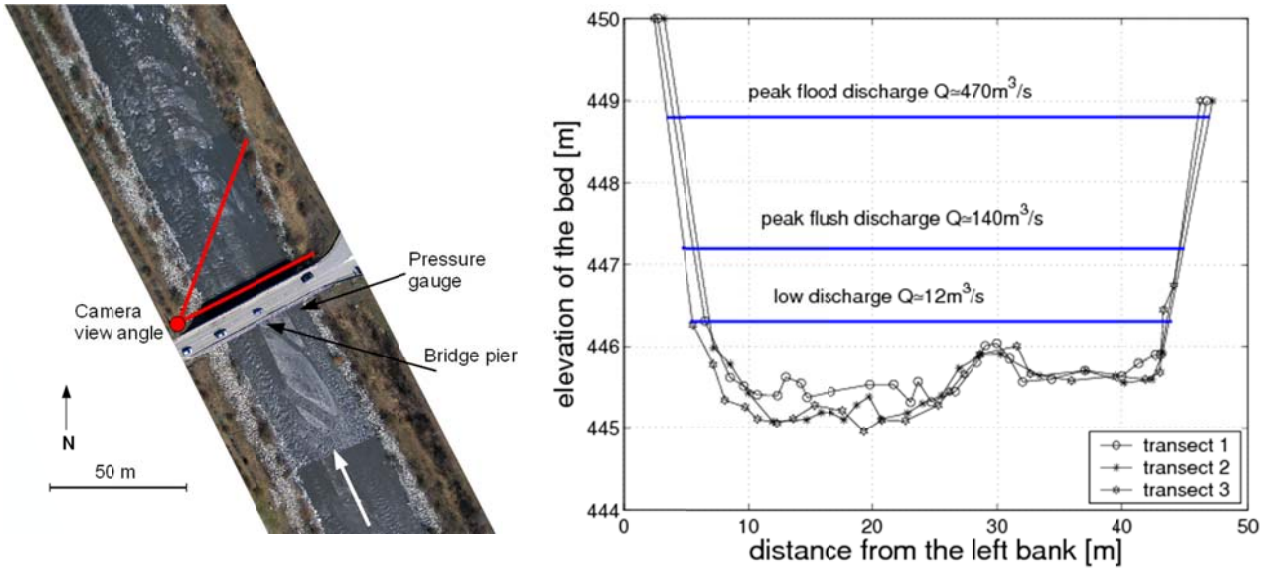

(a) (b)

Fig.3 LSPIV set-up in the test cross-section : orthorectified aerial photograph taken by drone in 2006 (Jodeau, 2007), camera position and image field, bathymetry transect (a); Bathymetry cross-sections used for LSPIV discharge computation and water levels reached for low flow conditions, for the flush peak, and for the flood peak (b)

Fig.3b shows the topography of the cross-section and different water levels for usual low flow, peak flush and peak flood discharges. Three bathymetry profiles were measured at the position of the camera one day after the 2009 dam flushing experiment. Their projections onto the spanwise direction are superimposed in Fig.3b. The cross sections were measured with a Leica TC305 total station . Section T1 (transect 1) was perpendicular to the flow, whereas T2 and T3 were more oblique with respect to the flow

Author-produced version of the article published in Journal of Hydro-environment Research 5 (2011) 301-312
The original publication is available at http://www.sciencedirect.com, doi:10.1016/j.jher.2010.12.005

(cf. Fig.8). The bathymetry was measured in June 2009 because wading across the Arc river is rarely possible and using a boat is impossible for safety reasons. The T2 cross section was used preferentially for LSPIV discharge computation because it is centred in the orthorectified images. A sensivity test with T1 and T3 is reported in section 4.3.

3.3 Pontamafrey gauging station (EDF)

The Pontamafrey gauging station (Fig.2b) operated by EDF yields the reference discharge measurements in the Lower Arc River. Water level is monitored by a pneumatic pressure gauge (Hydrologic). The gauging station is located upstream of a concrete sill which provides hydraulic control. Because the crest of the sill was refurbished in 2006, only a limited number of discharge measurements (so-called 'gaugings') are available to document the stage-discharge relationship (so-called 'rating curve').

Gaugings may be conducted either in the vicinity of the gauging station or at the LSPIV site located 7 km downstream, as no water input nor output occurs between both sites. To compare discharges measured at the LSPIV site with the discharges measured at Pontamafrey gauging station, the propagation time is estimated based on the mean gauged velocity. Propagation time usually ranges between 30 min and 1 hour. Discharge measurements are performed using current meters (electromagnetic Nautilus, Ott) and profilers (acoustic Streampro, RD Instruments). Between 10 and 80 m³/s, discharge data are missing, since the only available measurements were conducted with a Streampro and were discarded due to acoustic problems because of too high sediment concentrations.

During the 2008 flood rise and peak, intrusive hydrometric techniques were impossible to deploy due to high flow velocities and floating debris. During the flood fall, EDF hydrometry staff managed to deploy a van-mounted torpedo mechanical current-meter (80 kg, Ott C31, plastic propeller) from a bridge located 500 m downstream of the LSPIV site, along a wider section of the river, just downstream of the junction of the Arc River and the Glandon Torrent (Fig.2b). The contribution of this torrent during the flood was estimated to be less than 20 m³/s, roughly. The total gauged discharge, 380 m³/s, was the only gauged discharge above 140 m³/s.

After the refurbishment of the sill in 2006, the cross-section may be represented as three sills side by side (Fig.4b). EDF established a rating curve (Fig.4a) by regressing two conventional power laws against available gaugings, writing $Q=a(H-H_0)^b$, with Q, the discharge; H, the water depth, H_0 a reference water depth; and a and b, two calibration coefficients; the first power law is a sill formula (b=1.5) for the first sill of length L_1; the second power law is calibrated against available gaugings. The hydraulic control exerted by the sill supports the relevance of such a power law, but for the 2008 flood discharges, a system of three sills side by side must be considered. A simple formulation for the rating curve then writes:

$$Q=C\sqrt{2g}\left[L_1\left(H-\Delta z_0\right)^{3/2}+L_2\left(H-\Delta z_0-\Delta z_1\right)^{3/2}+L_3\left(H-\Delta z_0-\Delta z_1-\Delta z_2\right)^{3/2}\right] \quad (1)$$

with C a discharge coefficient (C=0.5); g, the acceleration of gravity; L_1=12.0 m, L_2=21.1 m, and L_3=14.5 m, the lengths of the three sills, Δz_0=-0.12 m, the staff gauge zero value; Δz_1=0.50 m, the level difference between the first and second sills; and Δz_2=0.50 m, the level difference between the second and the third sills. As can be observed in Fig.4a, Eq.1 yields very similar results to the rating curve established by EDF. Only for high water depths (over 2.5m), Eq.1 yields lower discharges compared to the EDF rating curve. The limits of Eq.1 are that the flow is not perfectly straight upstream of the sill (curvature of the channel at this location), the sills are not exactly horizontal and the third sill is partly protected by a spit 30 m ahead of the sill.

Author-produced version of the article published in Journal of Hydro-environment Research 5 (2011) 301-312
The original publication is available at http://www.sciencedirect.com, doi:10.1016/j.jher.2010.12.005

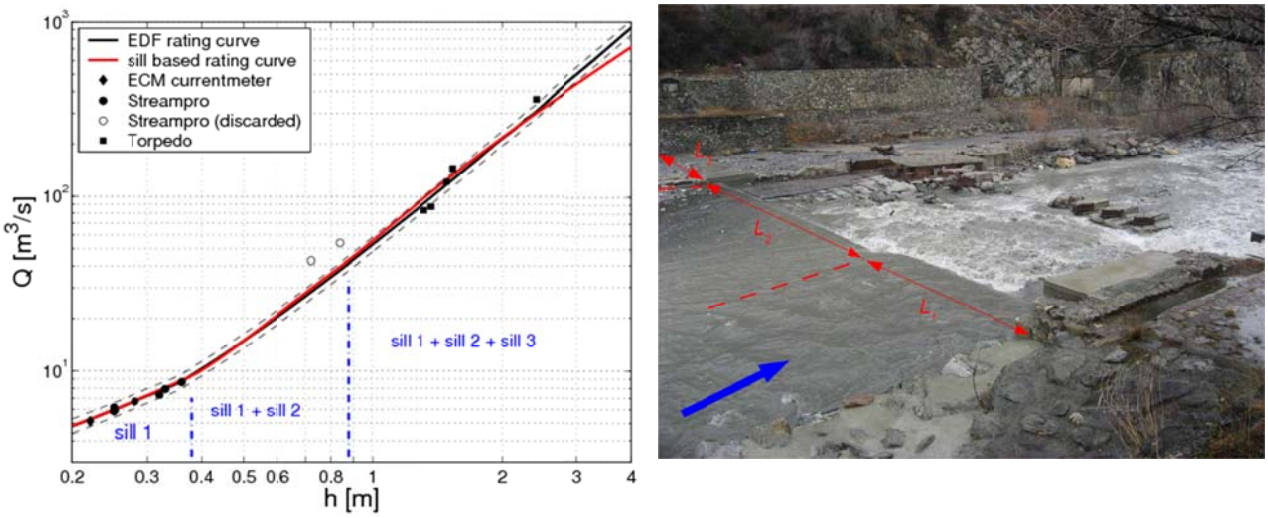

(a) (b)

Fig.4 Available gaugings, EDF rating curve (±10% in dashed lines) and sill-based rating curve (a, log scale); picture of the Pontamafrey gauging station showing the three sills during the 2009 dam flushing event (b).

3.4

3.5 Hydrological events (2008 flood and 2009 flush)

The hydrographs of the flood event in May, 2009 and of the flush event in June, 2009, together with LSPIV and gauging-van measurement times, are presented Fig.5. The flood event occurred in three phases with three increasing peak values. Only the third flood wave was measured using the LSPIV method from the rise to the peak of the flood on May 29th and during the fall on May 30th (Fig.5a).

The river dam flushing release obeys a typical hydrograph designed by the dam managers (Fig.5b): first, a warning wave comes early in the morning to prevent fish mortality; then, the discharge increases rapidly to 80 m^3/s with the opening of the dam gates; a relatively constant discharge is kept for three hours; a second increase of the discharge to the peak discharge (approximately 140 m^3/s) is produced by the release of water from most upstream mountain dams and lasts three hours approximately; the last part of the hydrograph corresponds to a relatively quick decrease of the discharge down to the compensation water. The DREAL (French Environment Regional Agency) hydrometry team proceeded to four discharge measurements with a gauging van during the flushing : two during the first plateau, and two during the second plateau for the peak discharge. The torpedo current meter was managed from a telescopic winch fixed in the van; the van was shifted for each vertical across the upstream side of the bridge (every three metres). Each of these gaugings lasted approximately one hour.

Author-produced version of the article published in Journal of Hydro-environment Research 5 (2011) 301-312
The original publication is available at http://www.sciencedirect.com, doi:10.1016/j.jher.2010.12.005

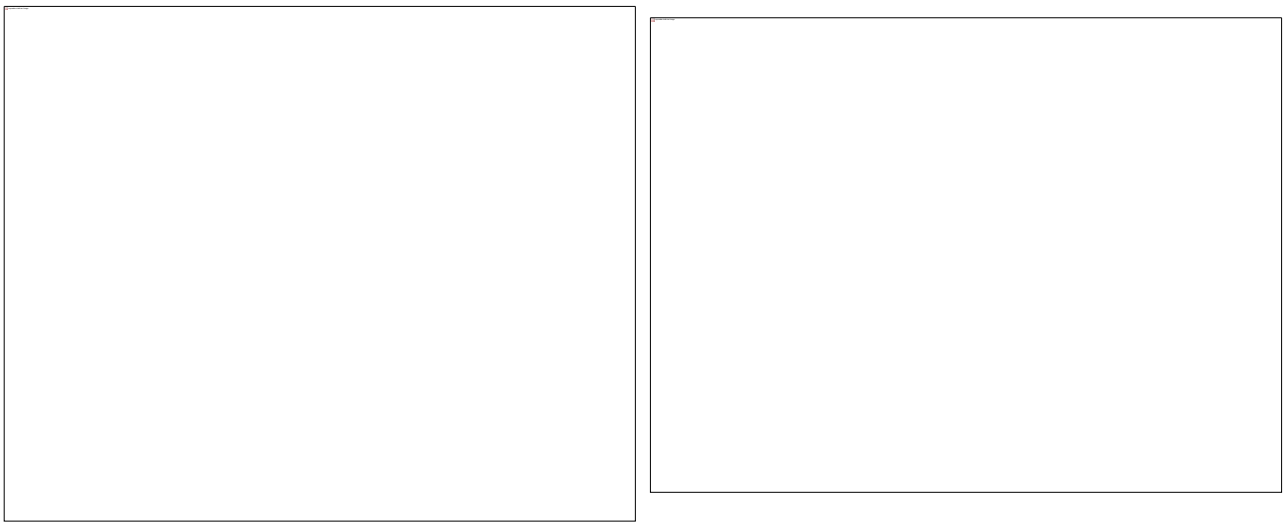

(a) (b)

Fig.5 Investigated hydrological events (a, 2008 flood and b, 2009 flush), LSPIV sequence times (red stars) and gauging-van measurement times (gray vertical rectangles). Water level records at Pontamafrey gauging station and at the LSPIV site are shown.

4 Results

4.1 Vertical velocity profiles

The velocity profiles measured during the flushing event using a torpedo current meter are presented in Fig.6. Measurements were performed at z=0.2h, 0.4h, 0.6h, and 0.8h, and for nine profiles at z=0.9h (solid circles in Fig.6). It appeared that data points were lacking especially close to the bed. Velocity profiles were completed adding virtual points (empty circles in Fig.6) at the surface (assuming a velocity at the surface equal to the velocity measured at the closest point from the surface) and near the bed (assuming a logarithmic profile close to the bed). The depth-averaged velocity u_m was computed for each profile using a linear interpolation of velocities. As observed previously by Jodeau et al. (2008) on the same site, the velocity profiles are particularly flat, which yields rather small values for the velocity coefficient α. The mean value from the experimental profiles equals 0.76 with a standard deviation equal to 0.05.

Dimensionless theoretical profiles were fitted to the data following Le Coz et al. (2010): a logarithmic profile fitted over the water depth h (dashed line) and truncated at 0.7h assuming a constant velocity over 0.7h. The best fit was obtained for a very high roughness height (k_s=1m) as small values were observed for the velocity coefficient α. This relatively large value for the roughness height may be explained by the contraction of the flow because of the bridge and also because of bedload transport (the mean dimensionless bed shear stress was estimated as θ_m=0.2, that is four times its critical value for the inception of motion). Camenen et al. (2006) or Recking et al. (2008) showed that the roughness height increases very fast as soon as bedload transport occurs. An estimation of the velocity coefficient may be obtained from the fitted theoretical profiles: using the logarithmic law, α=0.72; using the logarithmic law truncated at z=0.7h, α=0.79. These values border the estimation obtained directly from the experimental profiles. For the LSPIV calculation, the value α=0.76 will be used. The error in the discharge estimation due to the estimation of the velocity coefficient is thus ~7%. The uncertainty in the value of α may be larger if the LSPIV discharge computation has to be performed for other flow conditions, for instance at other locations in the river reach or for other discharge values.

Author-produced version of the article published in Journal of Hydro-environment Research 5 (2011) 301-312
The original publication is available at http://www.sciencedirect.com, doi:10.1016/j.jher.2010.12.005

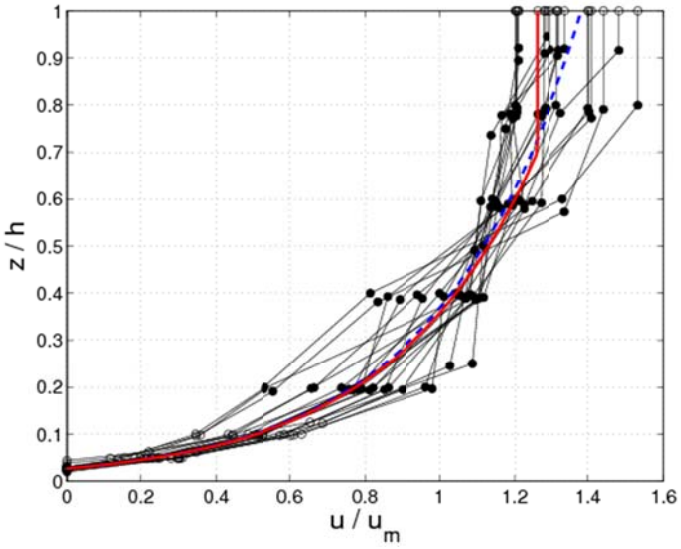

Fig.6 Dimensionless velocity profiles measured with a torpedo current-meter together with a logarithmic profile fitted over the water depth h (dashed line) and truncated at 0.7h assuming a constant velocity over 0.7h (solid line).

4.2 LSPIV parameterization and computations

As mentioned previously the image size is 720×576 pixels for all movies. The image sampling frequency depends on apparent water velocity and was adjusted to obtain pattern displacements of 15 pixels, which is an acceptable compromise to obtain a significant displacement of wel-correlated patterns. As the view points and velocity magnitudes were different for the flood and the flush events, two image sampling frequency values were defined (0.04 s and 0.2 s, respectively). Video sequences have variable quality, and some of them have sun reflection, shadows or waves when the water level is low. However, all the image sequences were used for LSPIV analyses.

Three positions of the camera were used in this study, one during the flush and two during the flood. During the flood the camera was put on a tripod and used with the largest side of the image along the width of the river. During the flush event the camera was set on the mast with the shortest side of the image along the width of the river.

The GRP distribution on the river sides was almost the same for both events. GRP positions are measured in the field and this positions were recalculated with the orthorectification matrix. The average position errors on all GRPs are 16 cm, 18 cm and 5 cm for the flush, flood (29 May) and flood (30 May), respectively. For some isolated GRPs located in the image far field, position errors may be as large as 30 or 40 cm.

In the orthorectification stage applied to correct the perspective effect, the chosen resolution is 0.01 m² for one pixel. The rectified image size is 450×500 pixels. For each sequence, all available images were used for LSPIV calculations. The LSPIV correlation is performed on squares of gray-scale pixels which are called Interrogation Areas (IA, cf. Muste et al. 2009). The maximum correlation search is restricted to a rectangular domain which is called Search area (SA), (Muste et al. 2009). For the flood and the flush processing data the same IA and SA were used. IA is a square of 12 pixels a side and SA is a rectangle 8×10 pixels with the longer side in the flow direction.

For all sequences, Tab.1 and Tab.2 present the water level in NGF and the LSPIV results with the discharge, the mean velocity and the wetted area. The results were presented in chronological order with the van discharge measurements. Deviations from the stage

Author-produced version of the article published in Journal of Hydro-environment Research 5 (2011) 301-312
The original publication is available at http://www.sciencedirect.com, doi:10.1016/j.jher.2010.12.005

discharge and the sill based curve were calculated. Fig.7 presents examples of time-averaged LSPIV surface velocity fields obtained with 2 LSPIV sequences.

The comparison of LSPIV discharge measurements with concurrent van-mounted torpedo measurements gives a valuable indication of the LSPIV discharge reliability and accuracy. However, LSPIV measurements lasted a few minutes whereas van measurements lasted 1 hour during the flush event and 2 hours during the flood event, approximately. The times indicated in Tab.1 and Tab.2 correspond to the beginning of each van measurement. Therefore, the flush LSPIV sequence (with addition of artificial tracers) following each van measurement must be considered, assuming that the instantaneous LSPIV discharge is representative of the 1-hour time-averaged van discharge. The deviations to van1 to van4 discharge values are 0%, -16%, +7%, -2%, respectively. It must be considered that the van2 discharge was measured during a period of time when the hydrograph was fastly falling and rising (cf. Fig.5b), which explains the large deviation. The comparison to the van5 discharge measured during the flood is more difficult, because a roughly estimated value of 20 m³/s accounting for the Glandon Torrent contribution must be withdrawn from the 380 m³/s gauged discharge. This is a minimum estimate of the Glandon discharge, which might have been greater in reality. The LSPIV discharge measurements at 8:45 (flood10) and 11:03 (flood11) are almost constant, with an average value of 330 m³/s. The resulting discharge deviation is -8%. From these comparisons, an average ±8% deviation between both techniques may be retained. As it is the usually recognized level of uncertainty for such velocity-area measurements (cf. ISO 748, 2002), it can be regarded as a maximum estimate of the LSPIV discharge uncertainty.

Author-produced version of the article published in Journal of Hydro-environment Research 5 (2011) 301-312
The original publication is available at http://www.sciencedirect.com, doi:10.1016/j.jher.2010.12.005

Tab.1 LSPIV sequences and gauging van measurements during the flushing event. LSPIV sequences with visible artificial tracers are indicated in gray boxes. The discharge deviation (%) is computed with the reference discharge yielded by the Pontamafrey gauging station (rating curve).

Name	Time (UT+1)	Water level (m NGF)	Q (m^3/s)	Q deviation (%) from EDF curve	Q deviation (%) from sill based curve	Mean velocity (m/s)	Wetted area (m^2)
flush1	2009/06/09 09:05	446.78	69	8.1	2.0	1.38	50
			71	11	1.4	1.43	
van1	2009/06/09 09:30	446.85	87	-12	-17	2.53	36
flush2	2009/06/09 09:55	446.88	83	21	14	1.54	54
			87	27	19	1.63	
van2	2009/06/09 10:25	446.79	83	-9.1	-15	2.51	33
flush3	2009/06/09 11:03	446.71	68	6.6	0.48	1.44	47
			70	9.7	3.4	1.49	
flush4	2009/06/09 12:45	447.03	111	21	13	1.87	59
			113	24	15	1.90	
van3	2009/06/09 12:50	447.03	121	3.5	-2.6	2.69	45
flush5	2009/06/09 13:37	447.10	127	15	7.8	2.05	62
			129	17	9.5	2.07	
van4	2009/06/09 14:00	447.12	144	15	8.7	3.10	47
flush6	2009/06/09 14:30	447.16	138	16	9.6	2.14	65
			141	19	12	2.19	
flush7	2009/06/09 15:30	447.06	117	1.5	-4.6	1.92	61
			124	7.5	1.1	2.03	
flush8	2009/06/09 16:28	446.80	74	-15	-21	1.47	51
			76	-13	-19	1.51	
flush9	2009/06/09 17:43	446.47	39	21	16	1.04	38
			41	27	22	1.08	

Author-produced version of the article published in Journal of Hydro-environment Research 5 (2011) 301-312
The original publication is available at http://www.sciencedirect.com, doi:10.1016/j.jher.2010.12.005

Tab.2 LSPIV sequences and gauging van measurements during the flushing event. LSPIV sequences with visible artificial tracers are indicated in gray boxes. The discharge deviation (%) is computed with the reference discharge yielded by the Pontamafrey gauging station (rating curve).

Name	Time (UT+1)	Water level (m NGF)	Q LSPIV (m^3/s)	Q deviation (%) from EDF curve	Q deviation (%) from sill based curve	Mean velocity (m/s)	Wetted area (m^2)
flood1	2008/05/29 10:02	448.42	365	-17	-8.5	3.03	120
			359	-19	-10	2.98	
flood2	2008/05/29 10:33	446.53	379	-19	-8.9	3.02	125
flood3	2008/05/29 10:52	448.46	372	-13	-3.8	3.03	123
flood4	2008/05/29 12:48	448.83	467	-7.3	5.2	3.34	140
flood5	2008/05/29 12:50	448.83	461	-17	-3.9	3.31	140
flood7	2008/05/29 14:10	448.79	463	-9.4	3.1	3.32	140
flood8	2008/05/29 17:36	448.80	462	-15	2.7	3.34	138
			462	-15	2.7	3.34	
flood9	2008/05/29 18:39	448.60	410	-22	-11	3.18	129
			407	-22	-11	3.16	
flood10	2008/05/30 08:45	448.13	337	0.8	5.0	3.14	107
			333	-0.42	3.8	3.11	
van5	2008/05/30 09:00	448.08	380	17	20	4.00	95
flood11	2008/05/30 11:03	448.05	322	7.4	9.5	3.11	104
			327	9.0	11	3.15	
flood12	2008/05/30 11:59	448.05	298	-0.63	1.4	2.87	104
flood13	2008/05/30 12:59	448.01	296	3.6	5.4	2.91	102
			292	2.2	4.0	2.87	

Author-produced version of the article published in Journal of Hydro-environment Research 5 (2011) 301-312
The original publication is available at http://www.sciencedirect.com, doi:10.1016/j.jher.2010.12.005

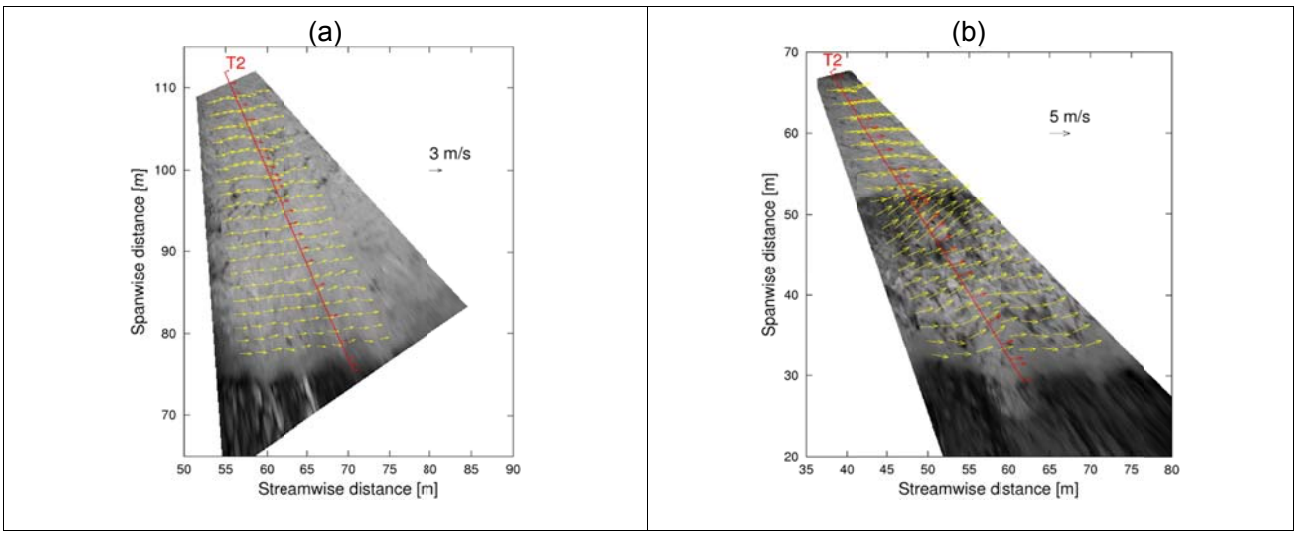

Fig.7 Examples of time-averaged LSPIV surface velocity fields: LSPIV sequences flush4 (a), flood7 (b).

4.3 Sensitivity tests and comparisons

Some sensitivity tests were conducted on parameters associated with the main identified sources of error in flood discharge measurements conducted with a mobile LSPIV system. These parameters are the water level used for image orthorectification and discharge computation, the number of image pairs used to establish the time-averaged LSPIV velocity field, the use of artificial tracers or not, the choice of the bathymetry cross-profiles amongst three possible transects in the same image. The effects of waves and free-surface deformation are also discussed. Sensitivity tests and comparisons are performed on a few representative LSPIV image sequences. Resulting discharge variations and deviations to both EDF and sill-based rating curves at the Pontamafrey gauging station are presented and further explained in the Discussion section.

Water level errors

Water level errors affect both the image orthorectification process, hence the velocities, and the wetted area computation from the bathymetry profile. The sensitivity tests were applied to the LSPIV sequence flood3 taken during the flood event. Similar results are observed with other sequences. For each LSPIV discharge computation, 100 images, i.e. 99 image pairs were processed. The water level was intentionally underestimated and overestimated by 10 and 50 cm. An error of 10 cm corresponds to a realistic water level error in flood conditions due to measurement errors and the water level variability in the orthorectified image plane. 50 cm corresponds to an extreme value when measurements are lacking and the water level is guessed from available information.

Tab.3 shows the simulated errors on the discharge, mean velocity and wetted area computed by LSPIV. As expected, the resulting errors for underestimated or overestimated water levels are symmetrical and of the same sign as the water level error. Discharge errors for a 10 cm water level error are less than 4%, which is negligible, for instance with respect to the velocity coefficient uncertainty estimated to be 7%, roughly. The variation in mean velocity is less than 1 cm/s (0.3%) and the variation in wetted area is about 5 m² (4%), which is consistent with a river width of 40 m, roughly. Discharge errors for a ±50 cm guess on the water level are ±18%, which would be a dominant source of uncertainty. Variations in wetted area still explain almost all the discharge variation: The variation in mean velocity, 2 cm/s (0.6%) is still negligible with respect to the variation in wetted area 23 m² (19%). In this study case, multiplying the water level error by the stream width therefore yields an accurate approximation of the LSPIV discharge error due to water level

Author-produced version of the article published in Journal of Hydro-environment Research 5 (2011) 301-312
The original publication is available at http://www.sciencedirect.com, doi:10.1016/j.jher.2010.12.005

error.

Tab.3 Simulated effect of different water level errors on the discharge, mean velocity and wetted area computed with the LSPIV sequence flood3 taken during the flood event (100 images processed). The gray box line indicates the reference computation.

Water level error (cm)	Q LSPIV (m^3/s)	Q deviation (%)	Mean velocity (m/s)	Wetted area (m^2)
0	376	0	3.07	123
-10	363	-3.5	3.07	118
+10	390	+3.7	3.07	127
-50	308	-18	3.09	100
+50	445	18	3.05	146

Waves and free-surface deformation

Quite high waves occurred during the 2008 flood, especially in the wake of the bridge pier. For some image sequences, this resulted in a marked deformation of the free-surface. The orthorectification of the images projected these 3D surface areas onto a horizontal plane. As a consequence, distorted velocity fields were obtained (Fig.7b, to be compared with Fig.7a, a flushing event sequence with much flatter surface). Typically, in the wave image area marked by darker pixels, LSPIV velocities appear deviated to the left. These directions are not consistent with visual observations of the flow during the flood. However, velocity magnitudes do not appear obviously biased and the cross-sectional velocity profile is regular.

Two main orthorectification errors may be induced by the presence of waves or free-surface undulations. First, the real water level is locally underestimated, which results in exaggerated horizontal distances and velocity magnitudes. However, as observed in the water level errors section, the velocity magnitude overestimation remains negligible, even for a 50 cm or 1 m high wave. Second, a positive or negative vertical velocity component due to the wave effect will be projected as a horizontal velocity component aligned on the camera viewpoint axis. In the present case, velocities going down the wave were interpreted as velocity components going to the camera, i.e., to the left side of the river.

The consequences for discharge computation are small because this effect is only local and because spanwise velocity components do not contribute to the flux across a bathymetry profile normal to the flow direction, which is nearly the case here. The dominant problem with 3D deformations of the free-surface is then the accuracy of the local velocity coefficient value, since the vertical velocity distribution may be complicated and different from the rest of the flow.

Image pair sampling

The time-averaged surface velocity field computed by LSPIV from an image sequence is affected by the number of image pairs processed, since random errors affecting individual velocity fields are reduced in the averaging process. From *N* consecutive images separated by a fixed time interval, *N*-1 image pairs can be processed. Tab.4 shows the LSPIV discharge and cross-section-averaged mean velocity results for the same LSPIV sequence flood3 and numbers of processed images varying from 2 (1 pair) to 2,247 (2,246 pairs). Similar results are observed with other sequences.

Author-produced version of the article published in Journal of Hydro-environment Research 5 (2011) 301-312
The original publication is available at http://www.sciencedirect.com, doi:10.1016/j.jher.2010.12.005

Few differences are observed when a sufficient number of image pairs are used to compute the average. In this case, processing 100 images is enough to reduce discharge variability to 1%. Of course, processing only a few images (<10) does not provide enough sampling information and may produce significant errors (-7% for 2 images) and scattered velocity fields. In this study, a few minutes of film were available for each sequence, usually from 500 to 3000 images were processed to establish the discharge. It corresponds to reasonable computation times (a few minutes) and to very short measurement durations, which is a decisive advantage of the LSPIV method for measuring fast flood events. In contrast, gauging van measurements lasted from 1 to 2 hours, during which time the river discharge may vary significantly.

Tab.4 Simulated effect of the number of processed images on the discharge and mean velocity computed with the LSPIV sequence flood3 taken during the flood event. The gray box lines indicate the reference computations for 100 images (variations less than 1%) and for 2247 images (reference results retained in this study).

Number of images *N* (*N*-1 image pairs)	Q LSPIV (m^3/s)	Q deviation (%)	Mean velocity (m/s)
2247	372	0	3.03
1000	373	+0.3	3.05
500	375	+0.8	3.06
100	376	+1.1	3.07
50	380	+2.1	3.10
20	380	+2.1	3.10
10	371	-0.3	3.03
5	358	-3.8	2.92
2	346	-7.0	2.83

Use of artificial tracers

In sections located a few hundred meters upstream of the study site, Jodeau et al. (2008) observed that surface velocities measured by a similar LSPIV system during a dam flushing event were significantly underestimated when artificial tracers were not visible in the image sequences. In shadow areas with poor contrast and in areas with specular reflections on stationary waves, Jodeau et al. (2008) applied an intensity threshold criterion to get accurate velocity measurements.

From Tab.1 and Tab.2 the LSPIV results with and without injected chips can be compared for the nine sequences taken during the flushing event and for six of the sequences taken during the flood event. For the flush sequences, results without artificial tracing appear slightly though systematically underestimated by -3.3% on average, individual bias ranging from -1.6% to -6.0%. For the flood sequences, deviations are smaller and more balanced, ranging from -1.5% to +1.6% with an average of +0.6%. Unexpectedly, differences in LSPIV results for image sequences with and without visible Ecofoam chips were found to be insignificant for the flood event. For the dam flushing event, the underestimation trend previously observed by Jodeau et al. (2008) is observed but is on average much smaller than the expected uncertainty in the velocity coefficient.

Author-produced version of the article published in Journal of Hydro-environment Research 5 (2011) 301-312
The original publication is available at http://www.sciencedirect.com, doi:10.1016/j.jher.2010.12.005

Cross-section bathymetry

Three bathymetry profiles were measured across the camera image after the 2009 flushing event. From a same time-averaged LSPIV surface velocity field, depth-averaged velocities can be computed at the points of the three different bathymetry profiles, T1, T2 and T3. Fig.8 shows an example of such a test conducted on the LSPIV sequence flush6 taken during the dam flushing event. Such a test could not be performed on a flood LSPIV sequence because bathymetry profiles T1 and T3 fall mainly outside the smaller orthorectified images. The middle profile T2 is the one used for all other discharge computations for both hydrological events.

As shown in Fig.3b, the projections of the three bathymetry profiles are similar with slight differences in the deepest part of the channel. Whereas T2 falls in the center of the image, profiles T1 and T3 sample velocity vectors located at the upstream and downstream ends of the LSPIV computational grid (Fig.8). Larger parts of profiles T1 and T3 fall outside the orthorectified image, hence the contribution of extrapolated velocities in the computed discharge is greater.

As expected, Tab.5 shows that from T1 to T3, i.e., with increasing angle between the bathymetry profile and the normal direction to the main flow, the wetted area increases whereas the mean velocity decreases. These opposite variations appear to more or less cancel one another out, since the discharge deviations to T2 results are -4.3% and -3.5% for T1 and T3, respectively. The underestimation trend might be explained by errors induced by the velocity extrapolation method applied (Le Coz et al., 2010). However, these deviations are acceptable for flood discharge measurements. Here again, they are smaller than the expected uncertainty in the velocity coefficient (~7%).

Tab.5 Results computed with LSPIV sequence flush6 using three different bathymetry profiles, T1, T2 and T3. The gray box line indicates the reference computation with the T2 bathymetry profile.

Cross-section bathymetry profile	Q LSPIV (m^3/s)	Q deviation (%)	Wetted area (m^2)	Mean velocity (m/s)
T1	135	-4.3	60	2.27
T2	141	0	65	2.19
T3	136	-3.5	67	2.02

Author-produced version of the article published in Journal of Hydro-environment Research 5 (2011) 301-312
The original publication is available at http://www.sciencedirect.com, doi:10.1016/j.jher.2010.12.005

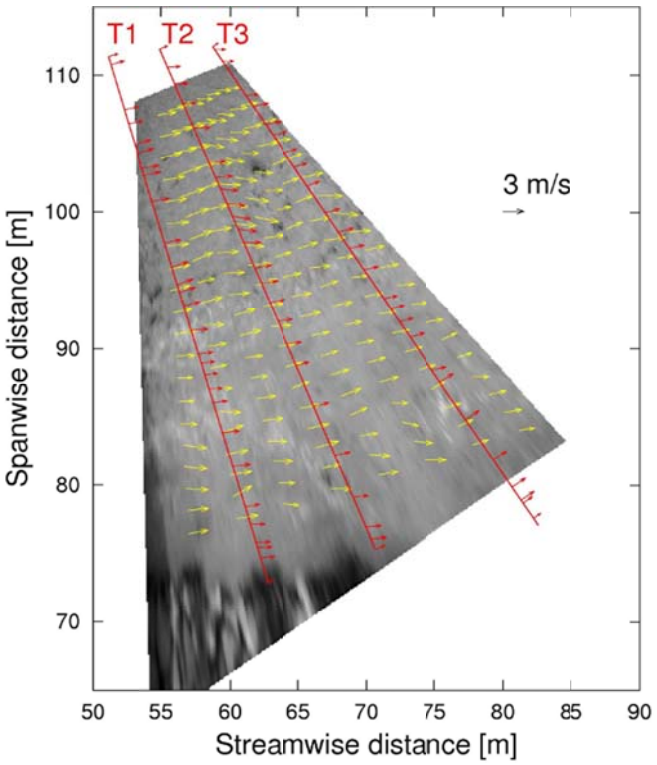

Fig. 8 Time-averaged LSPIV surface velocity field (yellow vectors) and depth-averaged velocities (red vectors) computed at the points of three different bathymetry profiles for the LSPIV sequence flush6 taken during the dam flushing event.

5 Discussion

5.1 Improvement of the stage-discharge relationship

The two stage-discharge relationships presented in section 3.3 are plotted in Fig.9 together with LSPIV measurements computed using the reference parameterization. It appears that LSPIV measurements are in agreement with the two relationships with a deviation less than 15%. LSPIV measurements carried out during the May 2008 flood draw a coherent stage-discharge relationship. Indeed, the sill-based rating curve yields a good prediction of the discharge when Q>300 m^3/s whereas the EDF rating curve seems to overestimate the discharge.

These results illustrate the decisive advantage of remote stream gauging techniques such as LSPIV measurements for improving the high-flow extrapolation of stage-discharge curves as also shown by Muste et al. (2010, this issue). As discharge measurements for infrequent floods are usually lacking, the extrapolation of rating curves is a necessary yet difficult exercise which leads to large uncertainties in discharge computations and flood percentiles (Lang et al., 2010). The consistency of high discharge LSPIV measurements with the simple sill-based hydraulic law confirms that this curve is more reliable than the fit previously performed by EDF on a few available gaugings. In this example, remote stream gauging LSPIV measurements show that rating-curve extrapolations based on hydraulic modelling, even as simple as sill hydraulic laws, yield better results than regression fits on available gaugings. In more complicated cases of gauging stations without a hydraulic structure or in the case where the flow is influenced by bridges, works or overbankflow processes, 1D or 2D hydraulic modelling may be required (Lang et al., 2010).

Author-produced version of the article published in Journal of Hydro-environment Research 5 (2011) 301-312
The original publication is available at http://www.sciencedirect.com, doi:10.1016/j.jher.2010.12.005

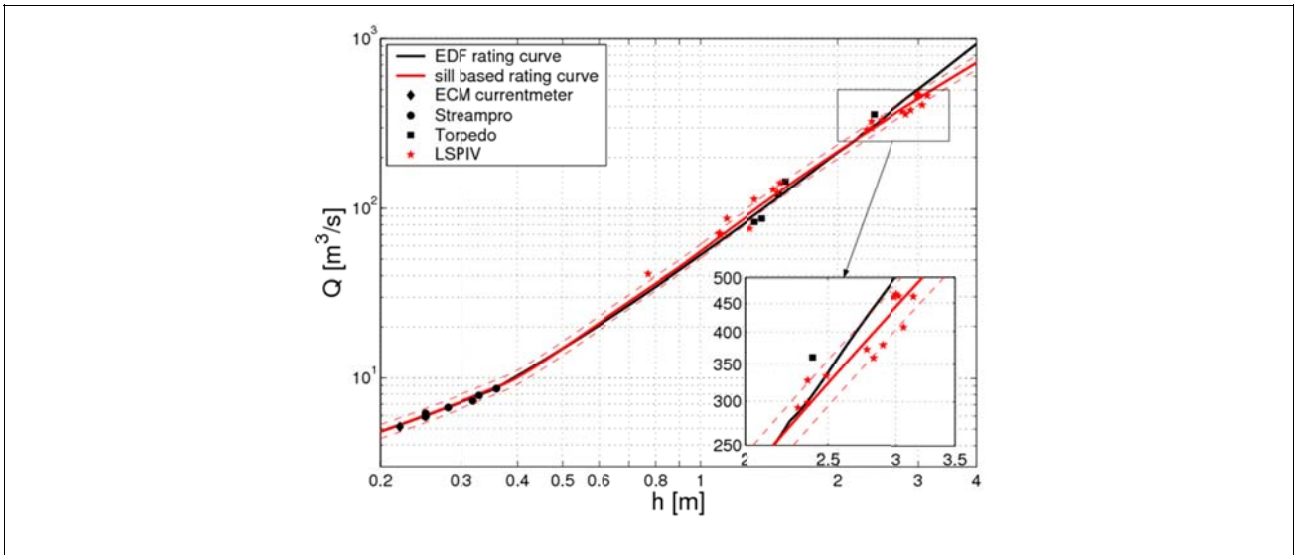

Fig.9 LSPIV flush and flood discharge measurements together with other available gaugings, the EDF rating curve and the sill-based rating curve (±10% in dashed lines). General view (a) and close-up view for highest discharges (b).

5.2 Dominant sources of errors and mean uncertainty

The comparisons to concurrent discharge measurements and the sensitivity tests conducted in this case study do not allow a precise quantification of flood discharge measurements obtained using a mobile LSPIV system. However, factual elements are brought to help discriminate dominant error sources, estimate mean uncertainty level, and prepare future detailed uncertainty analyses.

Our tests confirm that a reasonable uncertainty for mobile LSPIV discharge measurements conducted in favourable flood conditions is less than 10%, as already suggested by Le Coz et al. (2010). This is a performance equivalent to that of conventional velocity-area methods, which are usually considered to be accurate at a 5-10% level. However, this is an excellent score for high flood discharge values that cannot be gauged by conventional techniques and that are extrapolated with unacceptable uncertainties, most often. Moreover, the short duration of LSPIV image sequences (a few minutes) is a decisive advantage for gauging fast floods.

This study also confirms that the multiplicative error induced in LSPIV discharge computations by the velocity coefficient (cf. Le Coz et al. 2010) is a dominant source of uncertainty compared with other error sources. Much care must be paid to the site-specific mean value of the velocity coefficient (Muste et al., 2009). In the LSPIV literature, a default value was often considered (usually 0.85 from Rantz, 1982). The analysis of measured vertical velocity profiles using a log or a log-constant law is useful for establishing the values prevailing at a given study site, depending on the bed roughness and flow depth (cf. Le Coz et al. 2010). In the Arc river LSPIV site, both this study and that of Jodeau et al. (2008) found velocity coefficient values (0.72 – 0.79) smaller than the default value (0.85). In deeper river sections, Le Coz et al. (2007) and Le Coz et al. (2010) obtained velocity coefficient values as high as 0.90 with a ±0.05 variability. Therefore, ignoring the specific hydraulic conditions prevailing at a study site may lead to 10-15% errors on depth-averaged velocities and discharges.

Other sources of error explored in this study were found to be less detrimental than the velocity coefficient errors, with maximum deviations of the order of 5%, roughly. The effects of a typical water level error of 10 cm were found to be less than 5%. Provided a

Author-produced version of the article published in Journal of Hydro-environment Research 5 (2011) 301-312
The original publication is available at http://www.sciencedirect.com, doi:10.1016/j.jher.2010.12.005

minimal number of 10 images are processed, the effects of image pair sampling is less than 1%.

In our study case, the use of artificial tracers did not significantly improve the velocity measurements (mean deviation -3.3% during the flush, +0.6% during the flood).

Testing two bathymetry profiles in addition to the one that served as reference led to small discharge variations (-4%). All three profiles were measured after the dam flushing event. However, there is also a significant uncertainty in the exact bathymetry during the LSPIV measurements, especially during the flood. During major hydrological events, the bed may evolve significantly. One simple solution would be to measure bathymetry profiles before and after the event. However, as shown by El Kadi Abderrezzak and Paquier (2009), the maximum erosion depth during the peak discharge may be much larger than the depth before or after the event.

5.3 Practical guidelines for the application of mobile LSPIV flood measurements

Some useful recommendations can be drawn from this case study for the successful application of a mobile LSPIV system for flood discharge measurements or tests. They were showed in Tab. 6 with an evaluation of the factors influence .

Tab. 6 Recommendations for the mobile LSPIV measurements

	Recommendations / Steps	Importance
LSPIV velocity measurement	Straight and uniform reach	***
	Choice of the cross-section (piers...)	**
	The camera viewpoint and site angle	**
	The GRP measurement and distribution	****
	Seeding of artificial tracers	*
	Water level measurements	**
Discharge measurements using LSPIV	Water level measurements	****
	Bathymetry before/after the flood	**
	Choice of discharge transects	**
	Concurrent stream gauging	***
	Velocity coefficient	**

6 Conclusions

A mobile LSPIV system was successfully deployed during two hydrological events on the Arc River, a gravel-bed river of the French Alps: a flood greater than the 10-year return

period flood in May, 2008, and a reservoir flushing release in June, 2009. 36 image sequences with and without injection of artificial tracers were processed. For both events, LSPIV discharges fell within 8% of concurrent discharge measurements. During the flood peak, the mobile LSPIV system was the only stream gauging system that could be applied at this site due to the high surface velocities (up to 7 m/s) and floating debris.

This set of field data improves the knowledge and the uncertainty estimation of flood discharge measurement with a mobile LSPIV system. Sensitivity tests, comparisons and theoretical considerations were reported to assess the dominant sources of error in such measurements. The multiplicative error induced by the velocity coefficient was confirmed to be a major source of error.

The interest of LSPIV flood discharge measurements to improve the extrapolation of existing stage-discharge curves is demonstrated. A simple hydraulic law based on the geometry of the three sills of the Pontamafrey gauging station was proposed. The high flow LSPIV discharge measurements indicate that this new curve is more accurate for high discharges since they are evenly distributed in a ±10% interval around it. Remote stream gauging techniques such as LSPIV measurements offer the opportunity to gauge unfrequent floods, which are usually missed by conventional techniques. Together with the hydraulic analysis or numerical modelling of stage-discharge curves at gauging stations, they offer promising perspectives for improving our accurate knowledge of flood discharges.

7 Acknowledgements

Many hydrologists from different organizations have contributed to this study. They are deeply acknowledged, amongst others Alain Menant, Anne-Laure Besnier and Daniel Strippoli from EDF-DTG, Patrick Duby and Claire Godayer from DREAL, for their hydrometric measurements, Fabien Thollet and Mickaël Lagouy from Cemagref, for their involvement in the experimental work. The English manuscript was improved thanks to comments by Yves Dramais and Stephanie Moore.

8 References

ISO 748 (2007). Hydrometry - Measurement of liquid flow in open channels using current-meters or floats, ISO, 50 p.

Adrian, R. J., 1991. Particle-imaging techniques for experimental fluid mechanics. Annu. Rev. Fluid Mech., 23, 261-304.

Camenen, B., Bayram, A., Larson, M., 2006. Equivalent roughness height for plane bed under steady flow. Journal of Hydraulic Engineering, 132(11):1146–1158.

Cemagref and EDF-DTG (1998). Hydraulic study of the Arc de Maurienne River (phase 2). In French. Technical report, Cemagref and EDF-DTG, Lyon/Grenoble, France.

Costa, J., Cheng, R., Haeni, F., Melcher, N., Spicer, K., Hayes, E., Plant, W., Hayes, K., Teague, C., Barrick, D., 2006. Use of radars to monitor stream discharge by noncontact methods. Water Resources Research 42 (7), 14 p.

El Kadi Abderrezzak, K. & Paquier, A., 2009. One-dimensional numerical modeling of sediment transport and bed deformation in open channels Water Resources Res., 45, W05404, 20 p.

Fujita, I., Muste, M., Kruger, A., 1998. Large-scale particle image velocimetry for flow analysis in hydraulic engineering applications. Journal of Hydraulic Research 36 (3), 397–414.

Hauet, A., Creutin, J.-D., Belleudy, P., 2008a. Sensitivity study of large-scale particle image velocimetry measurement of river discharge using numerical simulation. Journal of Hydrology 349 (1-2), 178–190.

Hauet, A., Kruger, A., Krajewski, W. F., Bradley, A., Muste, M., Creutin, J.-D., 2008b. Experimental system for real-time discharge estimation using an image-based method. Journal of Hydrological Engineering 13 (2), 105-110.

Hydratec and Cemagref (1999). Hydraulic study of the Arc de Maurienne River from Modane to the Isère River, Morphology of the Arc River bed. In French. Technical report, Hydratec and Cemagref, Lyon, France.

Jodeau, M., Hauet, A., Paquier, A., Le Coz, J., Dramais, G., 2008. Application and evaluation of LS-PIV technique for the monitoring of river surface velocities in high flow conditions. Flow Measurement and Instrumentation 19(2), 117–127.

Jodeau, M., 2007. Morphodynamique d'un banc de galets en rivière aménagée lors de crues (*Gravel bar morphodynamics in an engineered river during high flow events*, in French). PhD Thesis. Claude Bernard University, Lyon I, France, 205 p.

Kim, Y., Muste, M., Hauet, A., Krajewski, W. F., Kruger, A., Bradley, A., 2008. Stream discharge using mobile large-scale particle image velocimetry: A proof of concept. Water Resources Research 44, W09502.

Lang, M., Pobanz, K., Renard, B., Renouf, E., Sauquet, E., 2010. Extrapolation of rating curves by hydraulic modelling, with application to flood frequency analysis, Hydrological Sciences Journal, 55 (6), 883–898.

Le Coz, J., Pierrefeu, G., Jodeau, M., Paquier, A., 2007. Mean vertical velocity profiles from aDcp river discharge measurement datasets, paper presented at 32nd Congress of IAHR, Int. Assoc. of Hydraul. Eng. and Res., Venice, Italy.

Le Coz, J., Hauet, A., Dramais, G., Pierrefeu, G., 2010. Performance of image-based velocimetry (LSPIV) applied to flash-flood discharge measurements in Mediterranean rivers, Journal of Hydrology, 394, 42–52.

Marnézy, A., 1999. The Arc River and its valley; anthropization and geodynamics of an alpine river within its catchment. In French. PhD Thesis, Joseph Fourier University, Grenoble I, France, 682 p.

Muste, M., Fujita, I., Hauet, A., 2009. Large-scale particle image velocimetry for measurements in riverine environments. Water Resources Research, 44, W00D19, doi:10.1029/2008WR006950.

Muste, M., Ho, H-C., Kim, D., 2010. Consideration on direct stream flow measurements using video imagery : outlook and research needs. Journal of Hydro-environment Research. (This issue)

Rantz, S. E., 1982. Measurement and computation of streamflow. Vol. 1, Measurement of stage and discharge, Water-Supply Paper 2175. U. S. Geological Survey, Washington.

Recking A., Frey P., Paquier A., Belleudy P., Champagne J.-Y., 2008. Feedback between bed load transport and flow resistance in gravel and cobble bed rivers. Water Resources Research, vol. 44, 21 p.